

Toughening mechanisms in modified epoxy resins with different crosslink densities

F. Lu¹, C. J. G. Plummer^{1,*}, W. J. Cantwell², H.-H. Kausch¹

¹ Laboratoire de Polymères, École Polytechnique Fédérale, CH-1015 Lausanne, Switzerland

² Department of Materials Science and Engineering, University, Liverpool L69 3BX, UK

Received: 17 April 1996/Accepted: 6 May 1996

Summary

Crack-tip deformation has been investigated in pre-cracked samples of core-shell rubber particle modified epoxy resins with different degrees of crosslinking. Light cross linking resulted in cavitation of the modifier, the formation of croids and extensive crack-tip yielding, whereas these deformation mechanisms were suppressed at room T in highly crosslinked specimens. A zone of particle debonding was observed in these latter at high T, but this appeared detrimental to the toughness. Indeed it was possible to increase the toughness in this case by oxygen plasma treatment of the modifier particles.

Introduction

High performance epoxy resins are increasingly used as matrices in a wide variety of aerospace-grade composite materials. Unfortunately, their high crosslink density often prevents widespread plastic flow in regions of high stress concentration, rendering them brittle under normal operating conditions. Nevertheless, the presence of well dispersed rubbery domains can promote the growth of multiple shear deformation zones in the matrix and may lead to significantly greater energy dissipation at crack tips than in the unmodified resin (1-8). It has also been shown that the rubber may cavitate in the vicinity of the crack-tip on loading (9, 10). In certain core-shell rubber-modified resins, the crack-tip region contains line arrays of cavitated particles running roughly perpendicular to the principal stress axis, referred to as "croids", whose formation precedes large scale shear yielding (11). In the systems investigated by us, the crack-tip failure mechanisms in the unmodified resin depend strongly on crosslink density (12, 13). The more crosslinking, the smaller the extent of deformation around the crack tip, and the lower the fracture resistance, as is well known from work on other epoxies (8, 14-16). The question to be addressed here is that of

* Corresponding author

how the degree of crosslinking influences microdeformation at crack-tips in the presence of a core-shell rubber modifier.

Polymer	Resin		Hardener			Procedure	Characterization	
	EPN1138	EPN1139	BA	CAT*	DDS		M_c	T_g (°C)
A	10g	90g	64g	0.16g	0g	K	1900	81
D	0g	100g	0g	0g	35g	L	150	198

Table 1 Materials: M_c is the approximate molecular weight average between crosslinks in $g\text{mol}^{-1}$; Procedure K: cure 2 hours at 140 °C and 2 hours at 180°C; Procedure L: cure 1 hour at 180°C and 2 hours at 210°C; CAT: 2-Ethyl-4-Methyl-Imidazole*

Experimental

The lightly crosslinked system 'A' was based on a mixture of the prepolymer epoxy phenolic novolac resins Araldite® EPN1138 and EPN1139 (supplied by Ciba-Geigy Ltd.) cured with bisphenol A (BA). The highly crosslinked system 'D' was based on the prepolymer EPN1139 cured with a diamino diphenyl sulfone (DDS) hardener. The molecular weight averages between crosslinks in Table I were deduced from the tensile modulus above T_g and the stoichiometry, these giving consistent results. Core-shell particles with an acrylic/styrene shell and a styrene/butadiene rubber core were used as a toughener. Ten phr (parts per hundred parts of resin by weight) of modifier were blended with systems A and D by mechanical stirring, to give systems "RA" and "RD" respectively.

Fracture tests using the compact tension and single edge notch bending geometries were conducted according to the European Structural Integrity Society (ESIS) protocol (17) (details of the specimen geometries and test conditions are given elsewhere (18)) After testing, transmission optical microscopy (TOM) was used to examine semi-thin sections prepared by polishing down of samples from the interior of the test pieces. Samples for transmission electron microscopy (TEM) were prepared by cutting a block with a 2 x 2 mm² cross-section from the area of interest. This was left in 4% osmium tetroxide (OsO₄)/water solution for 5 days at room temperature (RT), after which staining and fixation of the rubber particles was observed to a depth of approximately 1 µm (11, 19). Thin sections (50 - 70 nm) were microtomed parallel to the direction of crack propagation and perpendicular to the fracture surface (Reichert-Jung Ultracut E), and examined in a Philips EM300 TEM at 100 kV. Although the particles were well dispersed in the matrix macroscopically, their distribution was locally inhomogeneous, particularly in system RD, as will be apparent from subsequent micrographs, with a tendency for particle clustering. In RD, a small proportion of the particles was also present in the form of relatively large spherical agglomerations, which were present throughout the sample volume, but these were not thought to affect the fracture test results significantly.

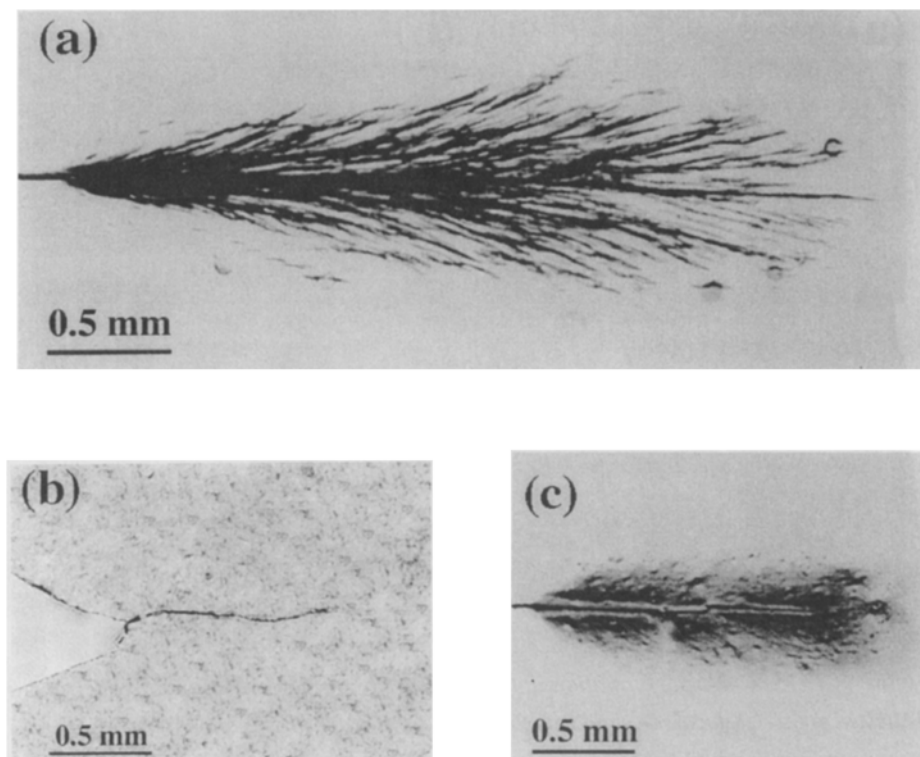


Figure 1. TOM of plane-strain crack tip damage zones: (a) system RA, tested at 60 °C; (b) system RD tested at 23 °C; (c) system RD tested at 160 °C.

Results and Discussion

In the lightly crosslinked modified system RA, multiple crack-like features were observed by TOM at the crack tip of specimens which had undergone sub-critical crack growth (Figure 1). These were seen at all T from RT to T_g , and optically resembled the 'croids' reported elsewhere in core-shell modified epoxies (11). The critical stress intensity factor (K_{IC}) was about 3.5 $\text{MPam}^{1/2}$ at RT decreasing to 3 $\text{MPm}^{1/2}$ close to T_g , which compares with values of about 1.3 $\text{MPam}^{1/2}$ in the unmodified resin. In the highly crosslinked modified system RD, on the other hand, TOM revealed no evidence of sub-critical damage at the crack tip in samples deformed at RT (Figure 3(a)), fracture being highly brittle, with $K_{IC} \sim 1 \text{ MPam}^{1/2}$ at RT, and rising slightly with increasing T to reach about 1.4 $\text{MPam}^{1/2}$ at 160 °C. In the unmodified resin $K_{IC} \sim 0.5 \text{ MPam}^{1/2}$ at RT, but increased more strongly with T than for the modified resin. Thus, at 160 °C, K_{IC} was slightly higher in the absence of the modifier. Paradoxically, then, it was only when T was raised to 160 °C that a small damage zone became visible by TOM in front of the crack tip in the modified resin (Figure 1(c)).

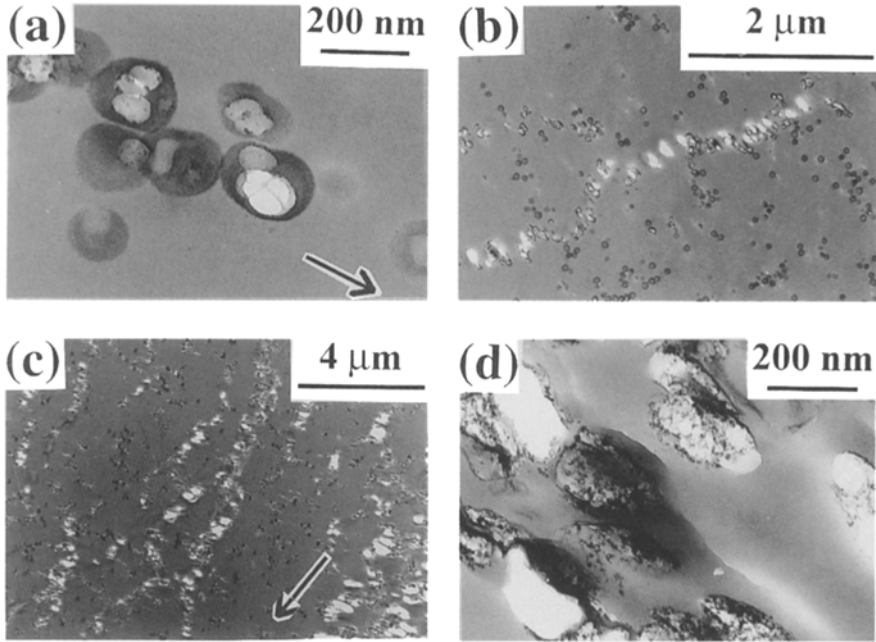


Figure 2. TEM of microdeformation in the outer regions of the crack-tip damage zone in RA tested at 60 °C (the arrows indicate the direction of crack propagation in each case): (a) cavitation of individual rubber particles; (b) early stages of croid formation; (c) denser croiding within the damage zone; (d) detail of the interior of a croid.

TEM of the crack tip region in material RA confirmed the features observed by TOM to consist of localized line arrays of cavities. As shown in Figure 2(a), taken from the periphery of the damage zone, the initial cavitation events were generally due to internal rupture of the particles. Once a given particle or group of particles has undergone cavitation the constraint release allows growth of the resultant hole in the matrix by plastic flow if the stress level is sufficiently high (20), leading to an increase in the extent of the triaxial stress concentration adjacent to the equatorial region of the hole. Thus localized regions of severe cavitation will tend to propagate roughly perpendicular to the principal stress axis (11, 21), as in Figure 2(b) for example, which was again taken from the periphery of the damage zone (note that for a constant applied stress, cavitation alone may not alter the local triaxiality significantly (22)). Work hardening will eventually stabilize the croid structure, although rupture of the ligaments between holes may also occur. Certainly Figure 2(c) suggests the croid structures to be coarser than would be expected based on cavitation of isolated particles, although it is difficult to distinguish between damage present prior to microtoming and that which was a direct result of microtoming. A contributing factor to both the irregularity of the croid structures, and to their tendency to break down may also be the inhomogeneity of the particle distribution.

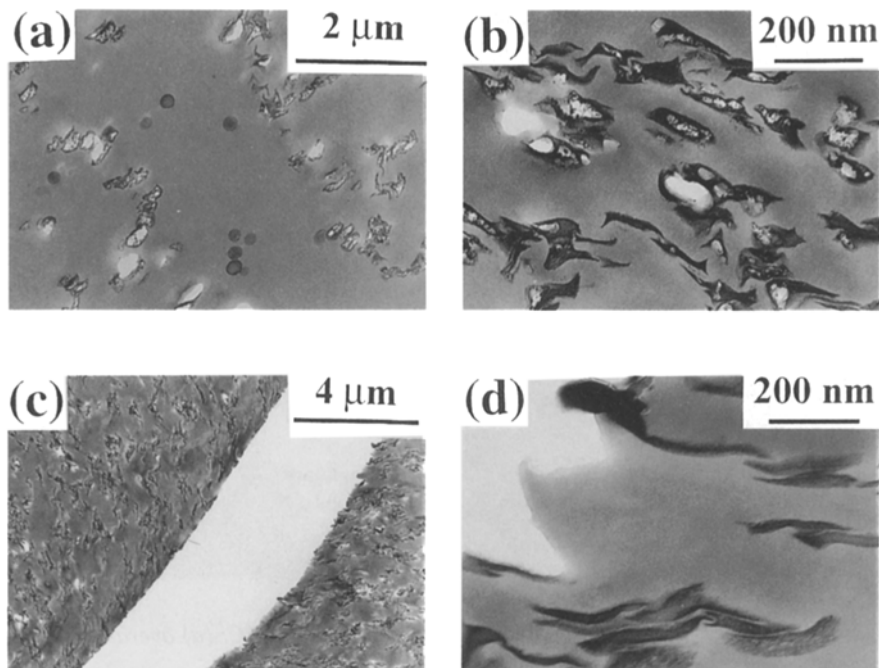


Figure 3. TEM of microdeformation in the inner regions of the crack-tip damage zone in RA tested at 60 °C: (a) the boundary of the zone of global shear; (b) detail of particle deformation; (c) deformation adjacent to the crack faces; (d) detail of (c).

Figure 2(d) shows a detail of Figure 2(c) showing elongated cavitated particles within a croid, indicating the extent of matrix shear deformation. In the outer regions of the damage zone, shear deformation was mainly confined to within the croids, i.e. to the ligaments separating the cavitated particles, but closer to the crack, there was a well-defined region in which severe deformation of isolated, non-cavitated particles was suggestive of a high degree of global shear deformation, as shown in Figure 3. The presence of a zone of global shear deformation close to the crack was consistent with TOM observations, a highly birefringent zone generally being seen adjacent to the crack-tip and crack faces.

In the highly crosslinked modified system RD, TEM of specimens deformed at RT confirmed the lack of cavitation and large-scale shear yielding at the crack tip inferred from TOM. Figure 4 is a TEM micrograph from the damage zone of Figure 1(c), obtained at 160 °C, where widespread cavitation was seen. As the micrograph suggests, the cavities tended to be associated with clusters of several particles, and their form was suggestive of debonding, and more particularly, debonding of the interface between adjacent particles (Figure 4(b)). The structures referred to as croids in the case of system RA were absent,

and indeed there was no extensive cavity growth. Moreover, even close to crack tip in system RD, isolated non-cavitated particles did not show the high degrees of deformation seen in RA, which indicates limited global shear deformation.

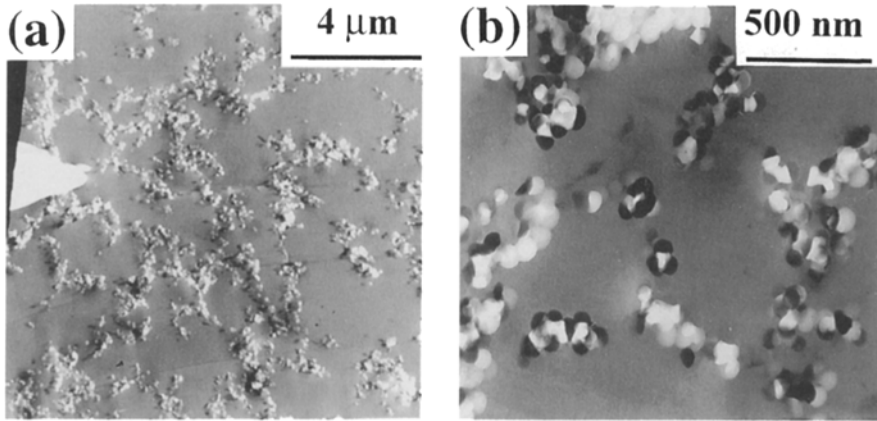


Figure 4. The crack-tip deformation zone in RD tested at 160 °C: (a) overall view of the crack-tip; detail of (a) from close to the crack-tip.

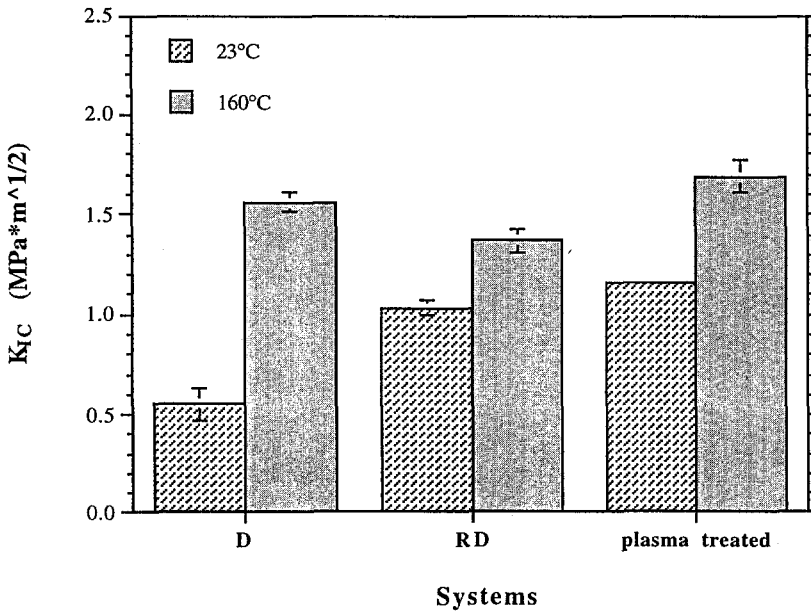


Figure 5: Comparison of the critical stress intensities of resin D, the modified resin RD and RD with plasma treated modifier particles, measured at two different temperatures

As mentioned previously, and as shown in Figure 5, although the inclusion of rubber particles resulted in a small increase in toughness at RT, as reflected by the K_{IC} results, at 160 °C there was a decrease in toughness in the modified specimens, in spite of the presence of a damage zone. Also shown in Figure 5 are the results of oxygen plasma treatment of the particles (18) which produced a substantial increase in K_{IC} at RT, and indeed a slight improvement over the unmodified specimens at high T. A subsequent examination of the fracture surfaces indicated that failure still occurred as a result of particle debonding, so that it may be possible to improve the high T toughness further by suitable surface treatments. The effectiveness of the surface treatment in this case suggests toughening may be due to crack-bridging by individual particles or particle clusters, although we have no direct evidence for this.

The lack of internal cavitation of the rubber particles in system RD may be linked to the poor particle dispersion (23), and it is therefore possible that cavitation could be induced by optimizing the particle (the plasma treatments described above were ineffective in this respect). However, it is not clear that this would be of great benefit for toughening, since cavitation itself contributes little to energy dissipation. It is far more significant that the RT yield stress in plane strain compression of the matrix in system RD is about 160 MPa, dropping to about 70 MPa at 160 °C, which compares with a RT value of 90 MPa in system RA. Under such circumstances the stress concentrating effect of the second phase (cavitated or uncavitated) may not be sufficient to induce yielding away from the crack-tip at the global stress levels required for brittle crack propagation. Moreover, the observed clustering of the particles and consequent increase in the *effective* interparticle separation may markedly reduce their effectiveness in synergistic mechanisms such as croiding. It is therefore noteworthy that from the observed K_{IC} and yield stress, the plastic zone size in resin D at RT is expected to be of the order of a few μm , i.e., approaching the cluster spacing in the modified system.

Conclusions

The failure mechanisms in two core-shell modified epoxy resins have been investigated by TEM. Croid formation, matrix shear yielding and the resultant crack tip blunting contribute to toughening in the lightly crosslinked modified system, as reflected by its relatively high K_{IC} . At low and intermediate T, no cavitation or croid formation occurred in the modified highly crosslinked system, and there was little evidence of widespread matrix shear yielding. At 160 °C the particles began to debond, primarily at particle-particle interfaces. This appeared to be detrimental to the toughness and indeed plasma treatment of the modifier particles in order to increase the interfacial strength resulted in a significant improvement in properties. Given the apparently deleterious effect of inter-particle contacts in this material, one of the causes of its diminished performance is likely to have been the poor particle dispersion, which also accounts for the lack of particle cavitation at low T.

Acknowledgements

This work was funded by Ciba-Geigy AG and the Fonds National Suisse.

References

1. McGarry, FJ (1970) *Proc. Roy. Soc. Lond.* A59: 68 .
2. Rowe, EH, Seibert, AR, Drake, RS (1970) *Mod. Plast.* 47: 110
3. Bascom, WD, Cottington, RL, Jones, RL, Peyser, P (1975) *J. Appl. Polym. Sci.* 19: 2545
4. Lange, FF (1973) *Phil. Mag.* 22: 983
5. Evans, AG (1972) *Phil. Mag.* 26: 1327
6. Bucknall, CB, Partridge, IK (1983) *Polymer* 24: 639
7. Yee, AF, Pearson, RA (1986) *J. Mat. Sci.* 21: 2462
8. Kinloch, AJ (1989) In: Riew, CK (ed) *Rubber-Toughened Plastics*, American Chemical Society, Washington DC (*Advances in Chemistry Series 222*, p 71)
9. Yee, FA, Li, D-M, Li, X-W (1993) *J. Mat. Sci.* 28: 6392
10. Pearson, RA (1990) Ph.D Thesis, University of Michigan
11. Sue, H-J (1992) *J. Mat. Sci.* 27: 3098
12. Lu, F, Cantwell, WJ, Kausch, H-H To be published in *J. Mat. Sci.*
13. Lu, F, Cantwell, WJ, Fischer, M, Kausch, H-H Submitted to *J. Mat. Sci. Lett.*
14. Pearson, RA, Yee, AF (1983) *Polym. Mater. Sci. Eng.* 49: 316
15. Pearson, RA, Yee, AF (1986) *J. Mat. Sci.* 24: 2571
16. Bradley, WL, Schultz, W, Corleto, C, Komatsu, S (1993) In: Riew, CK, Kinloch, AJ (eds) *Toughened Plastics I*, American Chemical Society, Washington DC (*Advances in Chemistry Series 233*, p 317)
17. European Structural Integrity Society test protocol for polymers (1992)
18. Lu, F (1995) PhD Thesis, EPFL
19. Sawyer, LC, Grubb, DT (1987) *Polymer Microscopy*, Chapman & Hall, London
20. Huang, Y, Kinloch, AJ (1992) *J. Mat. Sci. Lett.* 11: 484
21. Yee, AF, Pearson, RA (1989) In: Roulin-Moloney, AC (ed) *Fractography and Failure Mechanisms in Polymers and Composites*, Elsevier, London (p 291)
22. Huang, Y, Hunston, DL, Kinloch, AJ, Riew, CK (1993) In: Riew, CK, Kinloch, AJ (eds) *Toughened Plastics I*, American Chemical Society, Washington DC (*Advances in Chemistry Series 233*, p 1)
23. Sue, H-J, Garcia-Meitin, EI, Pickelman, DM, Yang, PC (1993) In: Riew, CK, Kinloch, AJ (eds) *Toughened Plastics I*, American Chemical Society, Washington DC (*Advances in Chemistry Series 233*, p 259)